TRANSPORT AND TELECOMMUNICATION INSTITUTE

The 16th International Conference

RELIABILITY and STATISTICS in TRANSPORTATION and COMMUNICATION (RelStat'16)

19–22 October 2016. Riga, Latvia

Organised by

Transport and Telecommunication Institute (Latvia)
in co-operation with
Latvian Academy of Science (Latvia)

PROCEEDINGS

Edited by

Igor V. Kabashkin

Irina V. Yatskiv

RIGA - 2016

Proceedings of the 16th International Conference *RELIABILITY and STATISTICS in TRANSPORTATION and COMMUNICATION* (RelStat'16), 19–22 October 2016, Riga, Latvia.

Papers were reviewed by the Scientific Committee members;
the responsibility for context and grammar of the papers rests upon the authors.

Transport and Telecommunication Institute
Lomonosova iela 1, LV-1019, Riga, Latvia
http://RelStat.tsi.lv

ISBN 978-9984-818-83-2

Proceedings of the 16th International Conference "Reliability and Statistics in Transportation and Communication" (RelStat'16), 19–22 October 2016, Riga, Latvia, p. 375–384. ISBN 978-9984-818-83-2
Transport and Telecommunication Institute, Lomonosova 1, LV-1019, Riga, Latvia

OPTIMISATION METHODOLOGY OF A FULL-SCALE ACTIVE TWIST ROTOR BLADE

Andrejs Kovalovs[1], Evgeny Barkanov[2], Sandris Ruchevskis[3], Miroslaw Wesolowski[4]

[1,2,3]Institute of Materials and Structures, Riga Technical University
Kipsalas St. 6B/6A, Riga, Latvia
[4]Department of Structural Mechanics, Koszalin University of Technology
Śniadeckich St. 2, Koszalin, Poland
Ph.: (+374) 29648795, e-mails: [1]andrejs.kovalovs@rtu.lv, [2]barkanov@latnet.lv,
[3]sandris.rucevskis@rtu.lv, [4]miroslaw.wesolowski@tu.koszalin.pl

This paper presents optimisation methodology for the design of the full scale rotor blade with an active twist to enhance its capability for vibration and noise reduction. This methodology is based on the 3D finite element model, planning of experiments and response surface technique to obtain high piezoelectric actuation forces and displacements with the minimal actuator weight and energy applied. To investigate an active twist of the helicopter rotor blade, the structural static analysis with thermal load using 3D finite element model was developed by finite element software ANSYS. Torsion angle obtained from the finite element simulation of helicopter rotor blades was successfully validated by experimental value to confirm the modelling accuracy.

Keywords: active twist, macro fibre composite (MFC), helicopter rotor blade, optimisation

1. Introduction

The traditional vibration reduction technique was a passive approach using, with vibration isolators and absorbers. However, this methodology imparts undesirable weight penalties and insufficient vibration reduction. Later, new control techniques were developed. This strategy involves active approach such as Higher Harmonic Control and Individual Blade Control. Disadvantages of this concept are adverse power requirements, limitation on excitation frequencies in HHC and extreme mechanical complexity of hydraulic sliprings in IBC (Shin *et al*., 2007). With an emergence of active materials, the Active Twist Rotor (ATR) concept was proposed. The actuators integrated and distributed into the rotor blade skin generate dynamic blade twist and camber adapted to the flight condition at any given time, which leads to significant vibration and noise reduction and improves flight performance.

The early studies are mostly experimental in nature with simple modelling and were undertaken to prove the concept of active twist control using piezoceramic materials. The key idea was to check ±2° of twist needed for suppressing vibration with minimum consumption of power. The first active twist rotor, using direct twist actuation, was developed by Chen and Chopra (1996). They built a Froude–scale model rotor blade with incorporated discrete dual-layer monolithic piezopatch elements embedded at +45° under the upper skin and -45° under the lower skin of the rotor blade. Different piezoceramic arrangements were analysed. The maximum twist at resonance frequencies were 0.35° and 1.1°.

With the emergence of piezo fibre technology the active twist concept was significantly improved. With this technology it is possible to create an active piezo ply within a composite laminate, such as Active Fibre Composites (AFC) and Macro Fibre Composites (MFC) actuators. The continuous piezo ply is structural more effective than the embedded monolithic piezo elements. Using the new actuator technology, a 1/6th Mach scale CH–47D blade model was built for wind tunnel testing at Boeing Helicopters (Philadelphia) with incorporated AFC (Rodgers *et al.*, 1997). Results of bench tests at frequencies up to 67.5 Hz demonstrated that a maximum twist of 1° to 1.5° peak-to-peak (pp) could be obtained.

In 1999, a joint venture from NASA, Army and MIT built and tested an active twist rotor with a structural design similar to the Boeing model rotor. Once more, the twist is generated by AFC actuators embedded into the rotor blade spar (Wilbur *et al.*, 2004). A four–bladed, aeroelastically scaled, ATR model was designed and fabricated to be tested in the heavy gas medium of a transonic wind tunnel to achieve better Mach–scale similarity. For the non–rotating results, the blade was mounted on the bench in a single–cantilevered condition. It was estimated that 1.1° to 1.4° maximum twist was generated for the 33–55 Hz frequency range at 1000 V electric excitation.

During a Collaborative research within the European Integrated Project "Integration of Technologies in Support of a Passenger and Environmentally Friendly Helicopter" (FRIENDCOPTER), twist blades were investigated more intensively. A series of blades was built using thin skin integrated actuators. At the first stage, several parameter studies for the optimisation of the skin lay-up were carried out (Riemenschneider *et al.*, 2004). Then demonstrator blades were designed and manufactured (Riemenschneider *et al.*, 2010). The baseline of the blade characteristics were taken from the well-known BO-105 model rotor blade. The actuators that were used are MFC, developed by NASA. These actuators are much more reliable than AFC actuators. In contrast to AFC, the rectangular PZT fiber of the MFC improved the maximum contact area between the PZT fibers and the interdigitated electrodes.

Cesnik and co–workers (2004a, 2004b) developed an optimisation framework to design an active blade that maximizes the static twist actuation while satisfying constraints on various blade requirements. The framework included UM/VABS for active cross section analysis, DYMORE for one dimensional geometrically exact beam analysis, a based cross–sectional parametric mesh generator and MATLAB's gradient based optimizer. Using the proposed design and manufacturing processes, the active twist rotor blade in model was designed and fabricated. Experimental structural characteristics of new rotor blade were compared with design goals and experimental results were compared well with modelling predictions. A maximum measured twist of 1.58°pp was reached at half of the operating voltage while all the actuators were working (Shin *et al.*, 2008).

The objective of the present study is development of the methodology, based on the planning of experiments and response surface technique, for the optimal design of active rotor blades using MFC actuators to obtain high piezoelectric actuation forces and displacements with minimal actuator weight and energy applied

2. Structure of helicopter rotor blade

The investigated full scale rotor blade with C–spar is based on the passive BO105 model scale rotor blade with C– spar and equipped with NACA23012 airfoils. The chord length c of 310 mm is in agreement with the original full scale rotor blade. Figure 1 shows the basic blade planform and cross–section dimensions selected for the full scale rotor blade. The blade is not pretwisted and the radius of this rotor is 4.9 m.

The investigated rotor blade consists of C–spar made of unidirectional Glass Fibre Reinforced Polymer (GFRP), skin made of ±45° GFRP, MFC actuators embedded into the skin, foam core and balance weight. The direction of piezoceramic fibres in MFC actuators coincides with the direction of the outside GFRP skin layers to maximize the twist actuation capabilities of the active plies on the top and bottom of rotor blade.

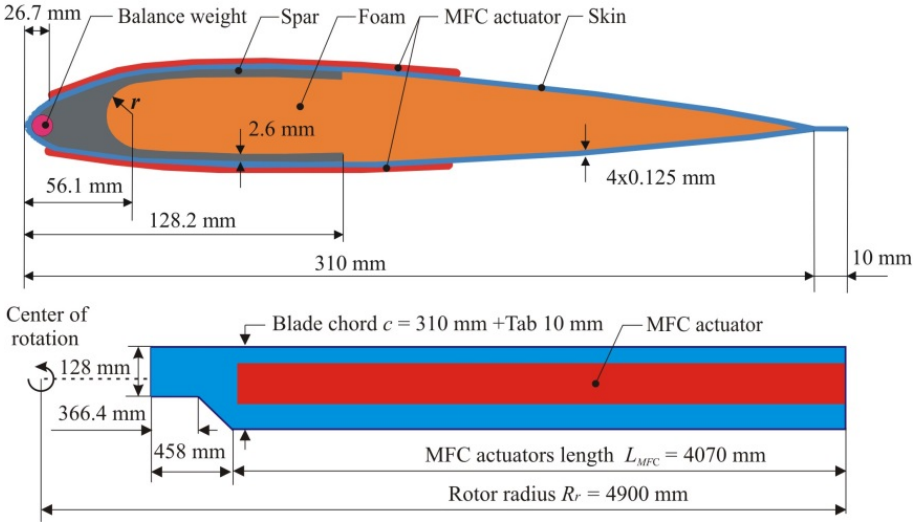

Figure 1. Cross–section and planform of the full scale rotor blade

3. Finite element simulation of helicopter rotor blade

In order to solve the optimisation problem of helicopter rotor blade with MFC actuators, the 3D finite element model of the rotor blade was modelled.

3.1. Finite element model

3D finite element model of the rotor blade is produced using commercial finite element software ANSYS 11.0, see Figure 2. It was comprised of two different types of finite elements: SHELL 99 and SOLID 186 which were used to model the different components of the blade. Some model simplifications were done, namely foam material was removed from the rotor blade tail. This gives the possibility to decrease the dimension of the finite element model and to preserve a proportional mesh for the blade skin without accuracy loss for the results obtained. Balance weight was modelled by volume element. The root is modelled by the linear layered structural shell elements SHELL99. The finite element model was constrained at the one side of the blade with a clamped boundary condition. The clamped condition was realized by putting the constraints on nodes, when all DOF's (degrees of freedom) are fixed.

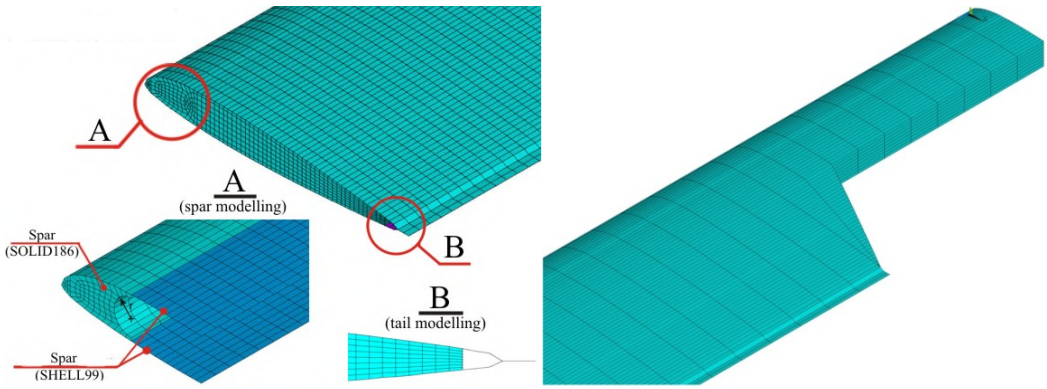

Figure 2. 3D finite element model of the rotor blade

3.2. Finite element analysis

To describe the behaviour of twisted rotor blade a structural static analysis is carried out to determine a torsion angle of the rotor blade, static torsion analysis to determine the location of the elastic axis and modal analysis to determine the first torsion eigenfrequency.

To determine the torsion angle the thermal analogy is involved in the static structural analysis. Thermal analogy between piezoelectric strains and thermally induced strains is used to model piezoelectric effects when piezoelectric coefficients characterizing an actuator are introduced as thermal expansion coefficients and voltage is equivalent to a temperature. The correspondence between piezoelectric strain and thermal strain is obtained by taking:

$$\alpha_{ij} = \frac{d_{ij}}{\Delta_{ES}}, \tag{1}$$

where d_{ij} is the effective piezoelectric constant and Δ_{ES} is the electrode spacing in MFC taken as Δ_{ES}=0.5 mm.

By using the actual piezoelectric properties for the proposed MFC actuator, it is possible to generate thermal analogy within ANSYS and to determine the torsion angle, see Figure 3. As the additional parameters the location of centre of gravity and the rotor blade mass are found from the finite element model.

Determination of the elastic axis location is more complicated problem and requires a solution of an additional static torsion problem with two forces applied independently from the both sides of the sought elastic centre. The modal analysis with block Lanczos mode-extraction method is used to determine the first torsion eigenfrequency. Convergence of the finite element results was examined for different meshes before optimisation study. From the results of mesh analysis, a finite element model with optimal number of elements was chosen for future calculations and research.

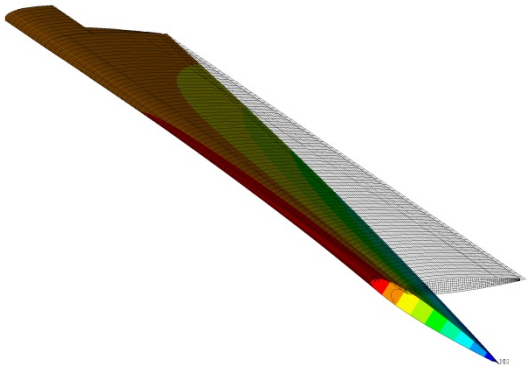

Figure 3. Twist of rotor blade

3.3. Experimental verification

Comparison of torsion angles for the 3D numerical simulation and experimental test of demonstrator blade was made to confirm the modelling accuracy. The demonstrator blade were designed and manufactured in DLR (Wierach *et al.*, 2013; Riemenschneider *et al.*, 2011). The main characteristics of this demonstrator were taken from the BO 105 model rotor blade. The chord length of 121 mm is in agreement with the original, whereas the profile was slightly changed into a symmetrical NACA 0012 due to the manufacturing reasons, which did not really change the blade from a structural point of view. The demonstrator is not pretwisted and the radius of this rotor blade is 1.74 m. The MFC actuator angle chosen for the present demonstrator is +40°, whereas the skin is made of unidirectional glass layers at an angle of –30°. To provide a good coverage with active material and to realize the desired actuation direction of +40°, special shaped MFC actuators were designed for the demonstrator blade. In total, six MFC actuators per skin were implemented. For measurements of active twist, the demonstrator blade was mounted on the test bed in a single cantilevered condition. The actuators were driven within a voltage range of –500V to +1300V with a quasi-static excitation of 0.15 Hz. Though a maximum of +1500V is allowed for the MFC actuators the actuation voltage was reduced to 1300V to avoid any electrical overload. The actuators were driven with a limited voltage of 1800Vpp. The angle of twist is in the order of 3.93°pp. The calculated twist rate, using piezoelectric actuation model developed here, is 2.94°pp/m over the length of the MFC actuators coverage (L_{MFC}).

Table 1 compares results of a finite element simulation with experimental test. It can be seen that difference between the experiment and simulation results of torsion angles is 3.2%. The comparison of the torsion angles between the experimental test and numerical result shows that the piezoelectric actuation model adequately predicts the static actuation performance by using the thermal analogy and confirms the modelling accuracy.

Table 1. Comparison of measured and calculated data

Title	Experimental result	Numerical simulation
Torsion angle φ, °pp	3.93	4.06
Twist rate φ/L_{MFC}, °pp/m	2.87	2.94

4. Design optimisation methodology

An optimisation methodology for the design of full-scale rotor blade with MFC actuators is based on the planning of experiments and response surface technique. The mathematical statement of the optimisation problem was described in details.

4.1. Optimisation methodology

Due to the large dimension of the numerical problem to be solved, an optimisation methodology is developed employing the method of experimental design and the response surface technique. The basic idea of this approach is that simple mathematical models (response surfaces) are determined only using the finite element solutions in the reference points of the experimental design. The significant reduction in calculations is achieved in this case in comparison with the conventional optimisation methods. The general flowchart of the optimisation methodology is shown in Figure 4.

In the first stage, a plan of experiments is produced in dependence on the number of design variables and number of experiments. In the second stage, the numerical model is created in order to model the response of a structure and then finite element analysis is performed in the reference points of the experimental design. In the third stage, the numerical data obtained by the finite element calculations in the sample points is used in order to build the approximating functions using the response surface method. These simple mathematical models obtained from the data of experiments are used as the objective functions and the constraints in the optimal design problem. The non-linear optimisation problem is executed by the random search method using the obtained response surfaces in the next stage. The optimal result of non-linear optimisation is checked using the finite element solution in the five stages. The optimal design variables are used in the numerical model in order to compare difference between the optimisation result and the numerical solution. If the difference between the optimal result and the finite element solution is higher than 5% it is needed to improve the correlations of the approximating functions or change of the design space for some parameters. The procedures are executed before obtaining the final optimal solution.

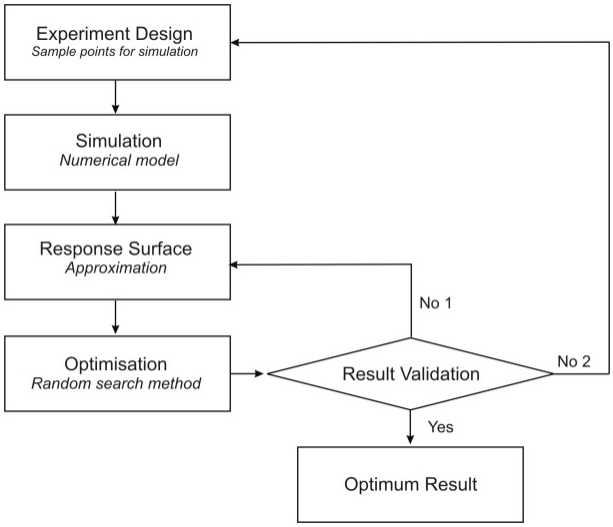

Figure 4. The flowchart of optimisation methodology for the designing of rotor blade

4.2. Experiment design

Auzins *et al.* (1977) suggested a non–traditional criterion for elaboration of the plans of experiments which is not dependent on the mathematical model of the object or process under consideration. The initial information for development of the plan is the number of variables n and the number of experiments k. The number of levels of factors (same for each factor) is equal to the number of experiments and for each level there is only one experiment. The points of experiments in the domain of factors are distributed as regular as possible. For this reason the following criterion is used:

$$\Phi = \sum_{i=1}^{k} \sum_{j=i+1}^{k} \frac{1}{l_{ij}^2} \Rightarrow \min \tag{2}$$

where l_{ij} is a distance between the points having numbers i and $j(i \neq j)$. Physically it is equal to the minimum of potential energy of the repulsive forces for the points with unity mass if the magnitude of these repulsive forces is inversely proportional to the distance between the points. Minimum of this criterion are being defined. The problem to minimize the criterion (Equation 2) leads to the solving of a non–linear programming problem. Solving the non–linear programming problem, the plans of experiments were determined for different number of the design variables n and number of the experiments k.

The plan of experiment is characterised by the matrix of plan B_{ij}. The domain of interest (domain of variables) is determined as $x_j \in [x_j^{min}; x_j^{max}]$, where x_j^{min} and x_j^{max} are the lower and the upper bounds of design variables, respectively. Thus, in this domain the sample points, where the experiments must be performed, are calculated by the expression:

$$x_j^{(i)} = x_j^{\min} + \frac{1}{k-1}\left(x_j^{\max} - x_j^{\min}\right)\left(B_{ij} - 1\right); \quad i = 1,2,...,k;\ j = 1,2,...,n \tag{3}$$

Since the matrices of plan B_{ij} are universal, these may be used for various design and optimisation problems. The program EDAOpt (Auzins *et al.*, 2014; Auzins *et al*., 2015) developed as a collection of non-gradient-based optimization software was used for the generation of the plan of experiment and simple random search optimisation method.

4.3. Response surface approximation

In 1981 Eglais (1981) proposed the algorithm of selection of the terms for non–polynomial regression function. In his work, the "correlation" approach for the optimal choice of the number of terms was also proposed.

In the present approach the form of the regression equation is unknown in advance. There are two requirements for the regression equation: accuracy and reliability. Accuracy is characterised as a minimum of standard deviation of the table data from the values given by the regression equation. Increasing the number of the terms in the regression equation, it is possible to obtain a complete agreement between the table data and values given by the regression equation. However, it is necessary to note that prediction in the intervals between the table points cannot be accurate.

For an improvement of prediction, it is necessary to decrease the distance between the points of the experiments by increasing the number of experiments or by decreasing the domain of factors. Reliability of the regression equation can be characterised by the affirmation that standard deviations for the table points and for any other points are approximately the same. Obviously, the reliability is greater for a smaller number of terms of the regression equation.

The regression equation can be written in the following form:

$$y = \sum_{i=1}^{p} A_i f_i(x_j) \tag{4}$$

where A_i are the coefficients of the equation of regression, $f_i(x_i)$ are the functions from the bank of simple functions $\varphi_1, \varphi_2,...\varphi_\kappa$ which are assumed as

$$\varphi_k(x_j) = \prod_{i=1}^{n} x_j^{\alpha_{ki}} \tag{5}$$

where n is the number of the object parameters and α_{ki} is a positive or negative integer including zero. Synthesis of the equation from the bank of simple functions is carried out in two stages: selection of perspective functions from the bank and then step-by-step elimination of the selected functions.

In the first stage, all variants are tested with the least square method and the function, which leads to the minimum of the sum of deviations, is chosen for each variant. In the second stage, the elimination is carried out using the standard deviation:

$$\sigma_0 = \sqrt{\frac{S}{k-p+1}}\ , \quad \sigma = \sqrt{\frac{1}{k-1}\sum_{i=1}^{k}\left(y_i - \frac{1}{k}\sum_{j=1}^{k} y_j\right)^2} \tag{6}$$

or correlation coefficient:

$$c = \left(1 - \frac{\sigma}{\sigma_0}\right) * 100\% \tag{7}$$

where k is the number of experimental points, p is the number of the selected perspective functions and S is the minimum sum of deviations.

If insignificant functions are eliminated from the regression equation, the reduction of the correlation coefficient is negligible. If in the regression equation only significant functions are presented, elimination of one of them leads to important decrease of the correlation coefficient.

4.4. Optimal design of full scale rotor blade

An optimisation problem for the optimum placement of MFC actuators in the full scale rotor blade is formulated on the results of parametric study of model scale rotor blade with C– spar (Glukhikh *et al*., 2008). The design variables of the rotor blade are shown in Figure 5. The actuation voltage was fixed at 1000V.

For the active twist optimisation of helicopter rotor blade, the objective function $f(x)$ is the torsion angle. Minimum and maximum bounds (domain of interest) for design variables are listed in Table 2. The lower and upper bonds of constraints for optimisation are given in Table 3. The constraints for the chordwise locations of the cross-sectional center of gravity and elastic axis are taken into account for aeroelastic stability. The constraints for the blade mass per unit span length and the first torsional frequency of the blade are accounted for a desirable blade dynamics.

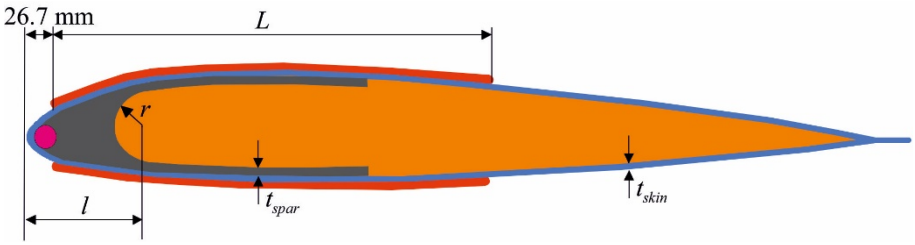

Figure 5. Design variables

Table 2. Domain of interest for optimisation

Title	Bounds
Spar circular fitting l, mm	$42.7 \le l \le 64.1$
Skin thickness t_{skin}, mm	$0.25 \le t_{skin} \le 1.25$
Spar thickness t_{spar}, mm	$1.34 \le t_{spar} \le 6.68$
MFC chordwise length L, mm	$42.7 \le L \le 267.0$

Table 3. Minimum and maximum bounds of the constraints

Title	Bounds
Centre of gravity location y_{cg}, %c	$y_{cg} = 30$
Elastic axis location y_{ea}, %c	$10 \le y_{ea} \le 25$
Blade mass per unit span length m, kg/m	$m \le 11$
First torsional frequency f_{T1}, Hz	$f_{T1} \ge 21$

The plan of experiments is formulated for 4 design parameters, namely, t_{spar}, l, t_{skin}, L and 30 experiment points. The plans of experiments in 3D view are presented in Figure 6.

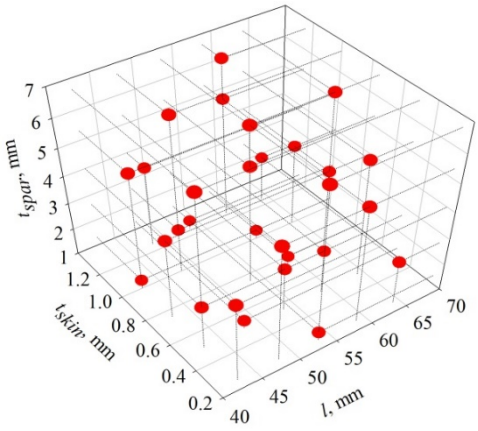

Figure 6. Plan of experiment: 3D–view

Subsequently in the points of plan of experiments the finite element solutions were obtained. In the next stage the numerical data obtained by the finite element calculations in the points of plan of experiments was used in order to build the approximating functions. Response surfaces for all behaviour functions were obtained with the correlation coefficients around 90% and higher. These response surfaces are verified by the finite element solutions in the points different from the points taken in the plan of experiments. Examples of finite element verification of the response surfaces of helicopter rotor blade are presented in Figure 7, where a very good correlation is observed for the approximations and finite element solutions. Non-linear optimisation problem was solved by the random search method using the response surfaces obtained in the corresponding program EdaOpt.

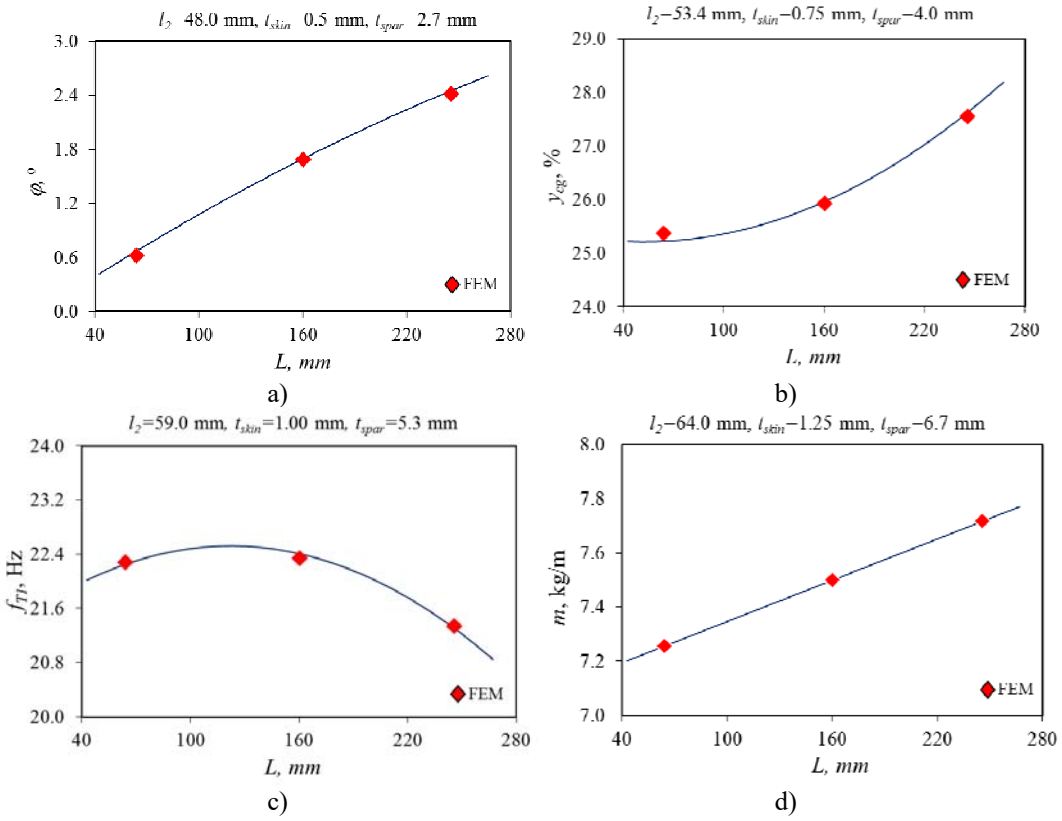

Figure 7. Accordance between approximations function and control points: (a) torsion angle, (b) center of gravity, (c) first torsion frequency, (d) mass per unit blade.

The optimisation results obtained for the full scale rotor blade are listed in Table 4. The maximum torsion angle is 1.78°, when the applied voltage is 1000V. Using the linear interpolation of the twist angle and taking the maximum voltage of $2000V_{pp}$, the maximum torsion angles reach 3.56°pp. The optimal results obtained with the response surface model (RSM) are verified by the finite element solutions (FEM). It is seen that these differences are very small. Mostly residuals do not exceed 2% that speaks about good correlation of the approximating functions.

Table 4. Optimisation results of full scale rotor blade

Title	Design variables				Constraints				Objective function
	l [mm]	t_{skin} [mm]	t_{spar} [mm]	L [mm]	y_{cg} [%]	y_{ea} [%]	m [kg/m]	f_{T1} [Hz]	φ [°pp]
RSM	47.7	1.0	3.7	258.0	30.0	23.8	6.1	21.1	3.56
FEM	47.7	1.0	3.7	262.0	29.9	23.6	6.1	21.0	3.62
Δ %	–	–	–	–	0.3	0.8	0	0.5	1.7

With the purpose to maximize a torsion angle, new constraints of the location of centre of gravity were studied additionally. During the preliminary study it was observed that the torsion angle obtained with the constraint when the location of centre of gravity y_{cg} =30%c is consistently lower than obtained

with the constraint y_{cg} =27.5…32.5%. Optimisation result with the new constraints is given in Table 5. The maximum torsion angle is 4.18°pp, when the maximum voltage is 2000V_{pp}. The comparative study of optimal results obtained for the full scale rotor blade with different constraints shows that the new constraints on the location of centre of gravity increases the torsion angle (14.8%) and decreases the blade mass per unit span length (6.6%). The minimal distance between the location of the centre of gravity and elastic axis saves the same for both constraints. The obtained results demonstrate that the new constraints are more effective.

Table 5. Optimisation results of full scale rotor blade with new constraint

Title	Design variables				Constraints				Objective function
	l [mm]	t_{skin} [mm]	t_{spar} [mm]	L [mm]	y_{cg} [%]	y_{ea} [%]	m [kg/m]	f_{TI} [Hz]	φ [°pp]
RSM	47.7	0.75	3.6	258.0	28.9	22.7	5.7	21.1	4.18
FEM	47.7	0.75	3.6	262.0	28.8	22.3	5.7	20.8	4.18
Δ %	–	–	–	–	0.4	1.8	0	1.4	0

For an individual blade control, the twist actuation amplitude of approximately ±2° is generally required as the minimum level of performance needed from the piezoelectric actuation. This level of actuation shows a good possibility for a vibration reduction (Wilkie *et al*. 1999). Figure 8 shows the relationship between the torsion angle and the required input voltage for two constraints. As one can see, to obtain the target actuation of ±2°, the optimal rotor blade requires 555V, when y_{cg} =30%*c* and 476V, when y_{cg} =27.5…32.5%.

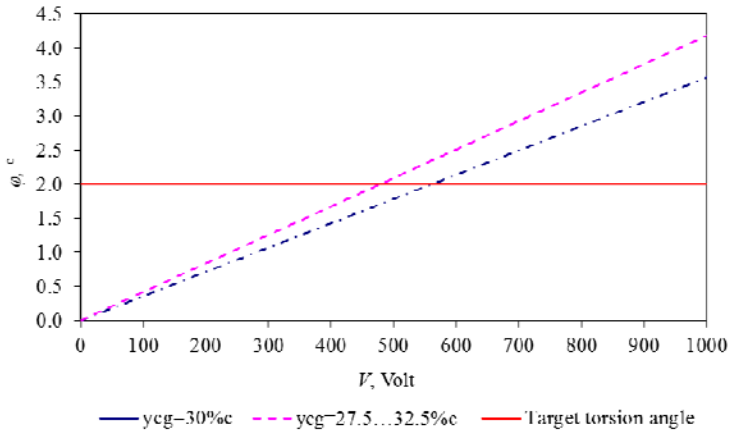

Figure 8. Minimized input voltage

5. Conclusions

The present investigations were carried out to develop new modelling and optimisation methodology for the design of helicopter rotor blades with an active twist to enhance its capability for the vibration and noise reduction. 3D finite element model of the helicopter rotor blade in the full scale was built according to the producer's requirements. The following general conclusions can be drawn based on the results presented in this work:

- To confirm the modelling accuracy, a comparison of the torsion angles between 3D numerical simulation and experimental test of the demonstrator blade was made. The demonstrator blade was designed and manufactured in DLR. The results of validation study show that the developed 3D finite element model based on the thermal analogy with a high accuracy predicts the static actuation performance of the helicopter rotor blades. To activate a piezoelectric effect in this model, the thermal analogy was used.
- The optimal design of the full scale rotor blade with was executed to show the capabilities of the developed optimization methodology. The optimal configuration of the full scale rotor blade was found for the twist actuation amplitude of ±2° required for an effective noise and vibration reduction in the helicopters.

Acknowledgements

Support for this work was provided by the Riga Technical University through the Scientific Research Project Competition for Young Researchers No. ZP-2016/17.

References

1. Audze, P., Eglais, V. (1977) New approach to planning out of experiments, *Problems of dynamics and strength* 35, 104–107 (in Russian).
2. Auzins, J., Janushevskis, A., Janushevskis J., Skukis E. (2014) Software EdaOpt for experimental design, analysis and multiobjective robust optimization, In: *International Conference on Engineering and Applied Science Optimization*, 4-6 June 2014, Kos Island, Greece, 14P.
3. Auzins, J., Skukis, E. Robust Optimization approach for Mixed Numerical/Experimental Identification of Elastic Properties of Orthotropic Composite Plates, In: *Proc. 6th Int. Conf. Coupled Problems in Science and Engineering*, 18–20 May 2015, Venice, Italy, 25 P.
4. Cesnik, C.E.S., Mok, J., Parekh, A., Shin S. (2004a) Optimisation Design Framework for Integrally Twisted Helicopter Blades, In: T*he 45th AIAA/ASME/ASCE/ASC Structures, Structural Dynamics and Materials Conference*, 19–22 April 2004, Palm Springs, USA, 10P.
5. Cesnik, C.E.S., Mok, J., Morillo, J.A., Parikh A.S. (2004b) Design Optimisation of Active Twist Rotor Blades, In: *30th European Rotorcraft Forum*, 14 – 16 September 2004, Marseille, France, 14P.
6. Chattopadhyay, A., Lin, Q., Gu, H. (1999) Modelling of Smart Composite Box Beams with Nonlinear Induced Strain, *Composite Part B: Engineering* 30(6), 603 – 612.
7. Chen, P., Chopra, I. (1996) Induced Strain Actuation of Composite Beams and Rotor Blades with Embedded Piezoceramic Elements, *Smart Materials and Structures* 5(1), 35 – 48.
8. Eglais, V. (1981) Approximation of data by multi–dimensional equation of regression, *Problems of dynamics and strength* 39, 120–125 (in Russian).
9. Glukhikh, S., Barkanov, E., Kovalovs, A., Masarati, P., Morandini, M., Riemenschneider, J., Wierach, P. (2008) Design of helicopter rotor blades with actuators made of a piezomacrofiber composite, *Mechanics of Composite Materials* 44(1), 77 – 86.
10. Riemenschneider, J., Keye, S., Wierach, P., Mercier des Rochettes, H. (2004) Overview of the Common DLR/ONERA Project 'Active Twist Blade', In: *30th European Rotorcraft Forum*, 14 – 16 September 2004, Marseille, France, 9P.
11. Riemenschneider, J., Opitz, S., Schulz, M., Plaßmeier, V. (2010) Active Twist Rotor for Wind Tunnel Investigations, In: *ASME 2010 Conference on Smart Materials, Adaptive Structures and Intelligent Systems*, September 28–October 1 2010, Philadelphia, USA, 19P.
12. Riemenschneider, J., Opitz, S. (2011) Measurement of twist deflection in active twist rotor, *Aerospace Science and Technology* 15(3), 216 – 223.
13. Rodgers, J.P., Hagood, N.W. (1997) Design, Manufacture, and Testing of an Integral Twist–Actuated Rotor Blade, In: *8th International Conference on Adaptive Structures and Technology*. 23 – 26 October 1997, Nagoja, Japan, 13P.
14. Sekula, M.K., Wilbur, M.L., Yeager, W. T. (1998) Aerodynamic Design Study of an Advanced Active Twist Rotor, In: *American Helicopter Society 4th Decennial Specialist Conference on Aeromechanics*, 1 – 3 June 1998, San Francisco, USA, 12P.
15. Shin, S.J., Cesnik, C.E.S., Hall, S.R. (2007) Design and Simulation of Integral Twist Control for Helicopter Vibration Reduction, *International Journal of Control, Automation, and Systems* 5(1), 24 – 34.
16. Shin, S.J., Cesnik, C.E.S., Wilkie, W.K., Wilbur, M.L. (2008) Design and Manufacturing of a Model–scale Active Twist Rotor Prototype Blade, *Journal of Intelligent Material Systems and Structures* 19(12), 1443–1456.
17. Wierach, P., Riemenschneider, J., Opitz, S., Hoffmann, F. (2013) Experimental Investigation of an Active Twist Rotor under Centrifugal Loads. *Adaptive, tolerant and efficient composite structures*. – Springer–Verlag Berlin Heidelberg.
18. Wilbur, M.L., Mirick, P., Yeager, W.E.A., Langston, C.W., Cesnik, C.E.S., Shin, S.J. (2004) Vibratory Loads Reduction Testing of the Nasa/Army/MIT Active Twist Rotor, *Journal of the American Helicopter Society* Vol.47(2), 123 – 133.
19. Wilkie, W.K., Wilbur, M.L., Mirick, P.H., Cesnik, C.E.S., Shin, S.J. (1999) Aeroelastic Analysis of the NASA/ARMY/MIT Active Twist Rotor, In: *55th Annual Forum of the American Helicopter Society*, 25 – 27 May 1999. Montreal, Canada, 13P.